

Is the Donor–Acceptor Electronegativity a Good Indicator for the Surface Enhanced Raman Scattering (SERS)?

Francisco J. Tenorio,^[a] Roberto Sato-Berrú,^[b] José M. Saniger,^[b] and Ana Martínez*^[c]

In this work, we study the interaction of neutral and ionic forms of Ag₈ and Au₈ with glycine to investigate the role of these interactions in the chemical enhancement (CE) component of the surface enhanced Raman scattering (SERS) effect. It is widely accepted that the charge transfer between metallic nanostructures and molecular species is a key issue in the underlying CE mechanism; consequently under this framework, and supported by the density functional theory, we introduce two recently described parameters, donor (χ^-) and acceptor (χ^+) electronegativity as useful concepts for the prediction of the charge transfer process

and the concomitant CE effect. From this work, it could be inferred that the minimum binding energy (BE) necessary for the CE to take place averages 30 kcal/mol. For the systems we present here, CE is more intense when BE is more negative and this occurs when there is a substantial charge transfer. Thus, as χ^- and χ^+ represent good parameters for analyzing the charge transfer process, they are also good indicators of the contribution of CE to the SERS effect. © 2012 Wiley Periodicals, Inc.

DOI: 10.1002/qua.24153

Introduction

Surface enhanced Raman scattering (SERS) effect was discovered decades ago.^[1] It has become an important analytical tool, as it has low detection limits, offers good selectivity for absorbates, responds well to the molecular environment and provides significantly improved vibrational signals. Owing to these characteristics, SERS has been applied extensively to various fields, including the trace analysis of biological molecules.^[2–15] In this sense, the interaction of metal nanoparticles with bio-molecules and microorganisms is evolving as an important field of research. In particular, several studies report many bio-molecules which interact with silver and gold.^[5,16–21] For example, the SERS spectra was used to determine the orientation of adenine, cytosine, and uracil at the surface of silver colloid,^[5] for the purpose of analyzing the bonding of 19-L amino acids on a silver surface,^[16] and to observe the effect of pH on the interaction of glycine (Gly) with gold and silver colloids.^[18] It has previously been reported that the intensity of SERS decreases when Gly interacts with silver colloid in an acidic environment (pH = 2). Apparently, the COOH group present at this pH does not interact strongly with the positively charged silver surface. Another investigation analyzing the interaction of lysine and gold colloids^[17] indicates that SERS intensity correlates with pH. These results suggest that the electrostatic interaction between the positive charge of the amino acid and the negative charge of the metal determines the SERS effect. An additional experimental and theoretical study^[19] used the SERS effect to analyze the tautomerism of thymine on gold and silver nanoparticles and to estimate energetic stability. Amino acids have not been the only object of investigation, certain peptides,^[20,21] and other bio-molecules such as sulfones,^[22] oligopeptides,^[23] methymazole,^[24] and paroxetine^[25] have also been used for the analysis of SERS.

After several years of investigation, it is now accepted that total enhancement can be understood in terms of two mechanisms^[26–28]: electromagnetic mechanism and chemical mechanisms [named chemical enhancement (CE)]. One of these chemical mechanisms is related to charge transfer transitions. Some authors^[18] affirm that certain chemical effects occur due to particular charge-transfer excitations and also as a result of other modifications to the electronic properties of the molecule which take place with absorption. Theoretical studies have been applied to investigate CE and some point to the presence of electrostatic attraction between the metal surface and certain molecules.^[18,21,24,27–29] These authors define some parameters that facilitate the characterization of the charge transfer process, related to the SERS effect. Several studies also use metal clusters as surface models.^[27–29] The evidence indicates that in fact the charge transfer between the metal and the molecule takes place in both directions, that is, from the metal cluster to the molecule and vice versa.^[28] The CE mechanism has also been characterized by applying the time-dependent density functional theory (DFT)^[29] when studying the interaction of pyridines with a small silver cluster (Ag₂₀). Apparently, CE does not correlate well with the magnitude of the

[a] F. J. Tenorio

Centro Universitario de Los Lagos, Universidad de Guadalajara, Jalisco 47460, México

[b] R. Sato-Berrú, J. M. Saniger

Centro de Ciencias Aplicadas y Desarrollo Tecnológico, Universidad Nacional Autónoma de México, Coyoacán 04510, Distrito Federal, México

[c] A. Martínez

Instituto de Investigaciones en Materiales, Universidad Nacional Autónoma de México, Coyoacán 04510, Distrito Federal, México
E-mail: martina@iim.unam.mx

Contract grant sponsor: PROMEP; contract grant number: 103.5/11/716.

Contract grant sponsor: SEP-CONACYT; contract grant number: 133316.

Contract grant sponsor: DGAPA.

© 2012 Wiley Periodicals, Inc.

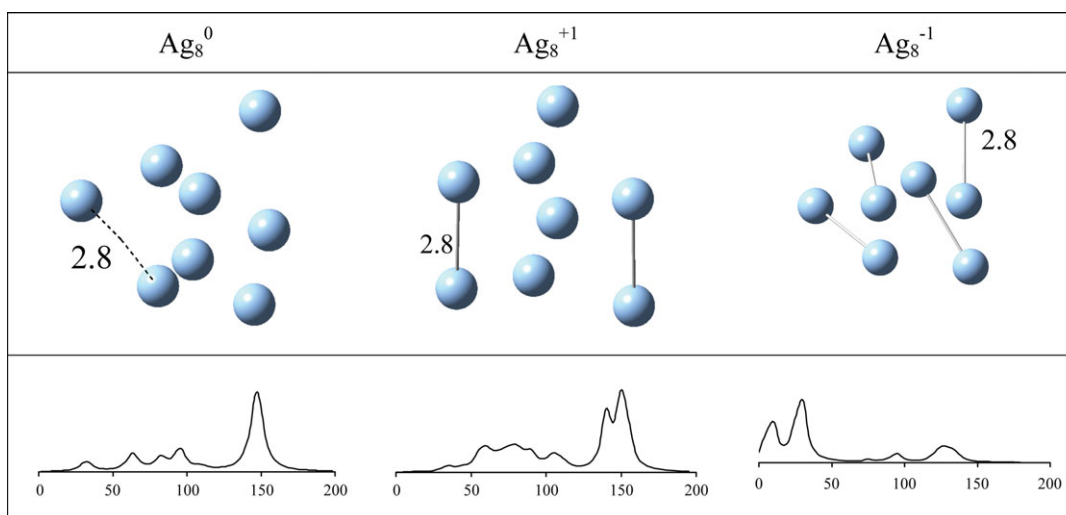


Figure 1. Optimized structures of Ag_8 (neutral, cation, and anion) and the corresponding Raman spectra are included. Intensity in arbitrary units. Selected bond distances (in Å) are also included. [Color figure can be viewed in the online issue, which is available at wileyonlinelibrary.com.]

charge transfer process. Instead, this phenomenon is governed by the energy difference between the highest occupied molecular orbital (HOMO) of the metal and the lowest unoccupied molecular orbital (LUMO) of the molecule. These results provide a possible explanation concerning the chemical mechanism involved in the SERS effect.

Despite all these reports, no studies have investigated how the electronic properties of the metals and molecules may influence the SERS signals, beyond the HOMO-LUMO gap. In this work, results for Ag_8 and Au_8 interacting with Gly are presented. The Raman spectra were obtained for Au_9Gly and Au_8Gly (neutral and ionic) to determine the CE in these systems. Because of the fact that the charge transfer process seems to be important for the CE of the signal, in this report, we propose two parameters, donor (χ^-) and acceptor (χ^+) electronegativity, which may predict the SERS effect. The main goal of this investigation is to analyze the electron donor-

acceptor properties of metal clusters and molecules, and for this purpose, a recently described new simple model based on DFT was applied.^[30] We used these chemical reactivity parameters to study the correlation between the charge transfer process and the CE of the SERS effect. Our results agree well with available experimental results, permitting us to conclude that these parameters are useful for the characterization of the charge transfer process and also for the prediction of CE. We were also able to establish the minimum binding energy necessary for the SERS effect to take place.

Computational Details

Density functional approximation^[31–33] as implemented in Gaussian 09^[34] was used for all calculations. Several initial geometries, considering three-dimensional and planar structures for the metal clusters and different bonding schemes for the

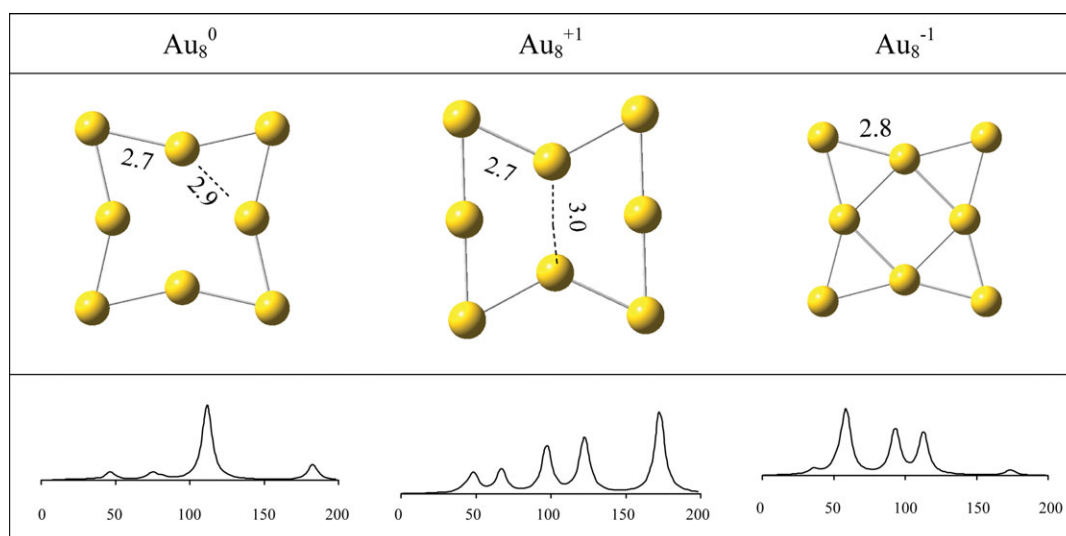
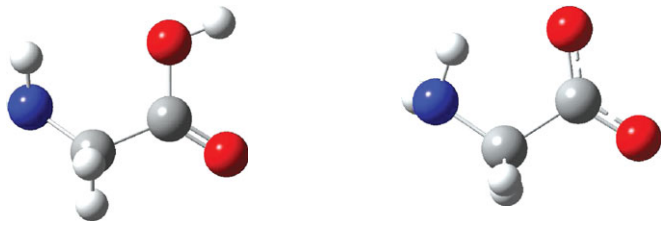


Figure 2. Optimized structures of Au_8 (neutral, cation, and anion) and the corresponding Raman spectra are reported. Intensity in arbitrary units. Selected bond distances (in Å) are also included. [Color figure can be viewed in the online issue, which is available at wileyonlinelibrary.com.]

Table 1. Optimized structures of Gly at different pH values. [Color figure can be viewed in the online issue, which is available at wileyonlinelibrary.com.]

Gly ⁺¹ (NH ₃ –CH ₂ –COOH) ⁺ pH < 2.35	Gly ⁰ (NH ₂ –CH ₂ –COOH) ^[a] 2.35 < pH < 9.78	Gly ⁻¹ (NH ₂ –CH ₂ –COO) ⁻ pH > 9.78
		
[a] Gly may exist as a zwitterion at the isoelectric point but in this work we considered the neutral Gly molecule as indicated in here since the optimization of the zwitterion fails.		

interaction of glycine with the metal clusters, were considered to perform full geometry optimizations without symmetry constraints. Frequency analysis including Raman spectra (calculated Raman scattering activities of the normal modes) were carried out for all the stationary points using the three parameters B3LYP^[35–37] density functional and the LANL2DZ basis sets.^[38–40] Harmonic frequency analysis allowed us to verify optimized minima. Local minima were identified by the number of imaginary frequencies (NIMAG = 0). Previous studies indicate that DFT reproduces equilibrium geometries and relative stabilities with hybrid functionals, which partially include the Hartree–Fock exchange energy. These results are largely consistent with those obtained using the Møller–Plesset perturbational theory at second order and basis sets of medium quality, such as 6-31G(d,p), and cc-pVDZ.^[41–43] As was reported before,^[44,45] the density functional approximation calculations

potential, μ . The chemical potential determines the charge flow direction and the capacity of the system to donate or accept charge. Gázquez et al.^[30] reported two different chemical potentials to distinguish the response to charge donation from the response to charge acceptance. They determined the following equations in terms of the vertical ionization energy (I) and vertical electron affinity (A), for the charge donation and the charge acceptance processes, respectively.

$$\mu^- = -\frac{1}{4}(3I + A) \quad (1)$$

$$\mu^+ = -\frac{1}{4}(I + 3A) \quad (2)$$

As the additive inverse of the chemical potential is the electronegativity (χ), from these equations, it is possible to define two different electronegativities for the charge transfer process: one that describes the donation (χ^-) and another one that is useful for the electron acceptance (χ^+).

$$\chi^- = \frac{1}{4}(3I + A) \quad (3)$$

$$\chi^+ = \frac{1}{4}(I + 3A) \quad (4)$$

It is important to emphasize that lower values of χ^- imply a better electron donor and larger values of χ^+ represent a greater capacity for accepting electrons. I and A refer to one electron transfer processes whereas χ^- and χ^+ consider fractional charge transfer reactions. In most of the reactions with gold neutral clusters there is a partial electron transfer. Because the partial charge transfer is one of the main intermolecular factors that dominates the binding energies in gold clusters, χ^- and χ^+ will be better parameters than I and A to describe the electron donor acceptor properties of these systems.

Results and Discussion

The optimized geometries of metal clusters (neutral, cation, and anion) are presented in Figures 1 and 2. The most stable

Table 2. Binding energies (in Kcal/mol) for the reaction between metal clusters and Gly, with different molecular charges.

Metal cluster	Chemical reaction	Binding energies (kcal/mol)
pH < 2.35	Ag ₈ ⁰ + Gly ⁺¹ → [Ag ₈ Gly] ⁺¹	-17.5
	Ag ₈ ⁺¹ + Gly ⁺¹ → [Ag ₈ Gly] ⁺²	[a]
	Ag ₈ ⁻¹ + Gly ⁺¹ → [Ag ₈ Gly] ⁰	-91.5
	Au ₈ ⁰ + Gly ⁺¹ → [Au ₈ Gly] ⁺¹	-19.9
	Au ₈ ⁺¹ + Gly ⁺¹ → [Au ₈ Gly] ⁺²	+29.9
	Au ₈ ⁻¹ + Gly ⁺¹ → [Au ₈ Gly] ⁰	-86.9
2.35 < pH < 9.78	Ag ₈ ⁰ + Gly ⁰ → [Ag ₈ Gly] ⁰	-1.5
	Ag ₈ ⁺¹ + Gly ⁰ → [Ag ₈ Gly] ⁺¹	-27.9
	Ag ₈ ⁻¹ + Gly ⁰ → [Ag ₈ Gly] ⁻¹	-5.8
	Au ₈ ⁰ + Gly ⁰ → [Au ₈ Gly] ⁰	-20.4
	Au ₈ ⁺¹ + Gly ⁰ → [Au ₈ Gly] ⁺¹	-38.7
	Au ₈ ⁻¹ + Gly ⁰ → [Au ₈ Gly] ⁻¹	-8.1
pH > 9.78	Ag ₈ ⁰ + Gly ⁻¹ → [Ag ₈ Gly] ⁻¹	-46.6
	Ag ₈ ⁺¹ + Gly ⁻¹ → [Ag ₈ Gly] ⁰	-131.7
	Ag ₈ ⁻¹ + Gly ⁻¹ → [Ag ₈ Gly] ⁻²	+14.9
	Au ₈ ⁰ + Gly ⁻¹ → [Au ₈ Gly] ⁻¹	-61.1
	Au ₈ ⁺¹ + Gly ⁻¹ → [Au ₈ Gly] ⁰	-148.1
	Au ₈ ⁻¹ + Gly ⁻¹ → [Au ₈ Gly] ⁻²	+13.2

[a] The compound of Gly⁺¹ with Ag₈⁺¹ was not possible to obtain as the atoms are not bonded after the optimization, possibly because the strong electrostatic repulsions between positive atoms.

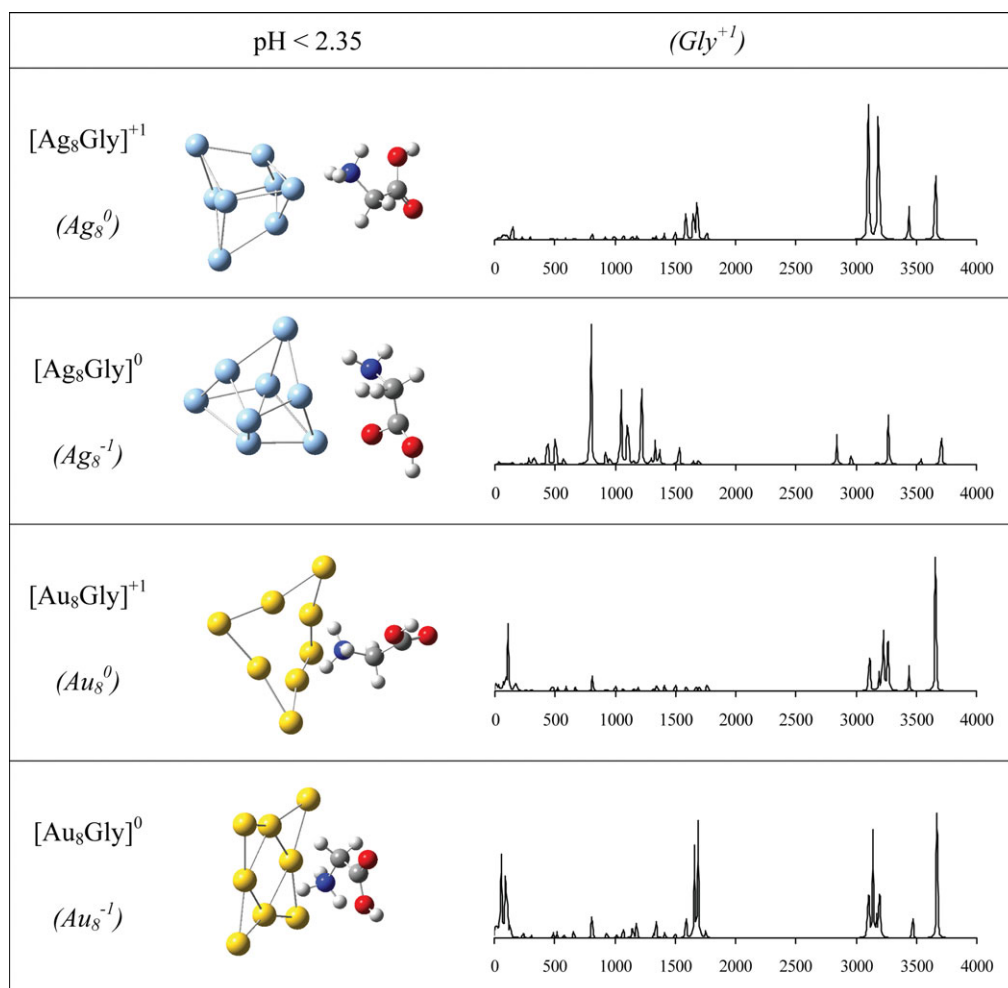


Figure 3. Optimized structures and simulated Raman spectra of Gly⁺¹ with Ag₈ and Au₈ (neutral, cationic, and anionic). Intensity of the Raman spectra in arbitrary units. [Color figure can be viewed in the online issue, which is available at wileyonlinelibrary.com.]

Ag clusters are tridimensional, whereas for Au clusters, they are planar. The optimized structures of Au₈, Au₈⁻, and Au₈⁺ were described previously^[46] and we reoptimize them in this investigation, to analyze the interaction of these clusters with Gly.

In this investigation, Gly was considered to be a cation, assuming that the environment was acidic (pH lower than the first pK_a, that is, equal to 2.35), neutral considering the pH between 2.35 and 9.78, and Gly⁻¹ so that the bonding scheme can be observed when the pH is higher than the second pK_a of Gly. The optimized structures for Gly at different pH values are presented in Table 1.

The Raman spectra for Gly do not depend on the pH. Both the calculated and experimental Raman spectra are similar at different pH values (see Supporting Information Figs. 15 and 25). Contrastingly, the Raman spectra of the metal clusters do depend on the global charge of the cluster, as shown in Figures 1 and 2. In cations, bands exist at higher frequencies than they do for anions. Ag₈ neutral spectrum is similar to the spectrum of Ag₈⁺¹, unlike gold clusters, as the spectrum of Au₈ is different to the spectrum of the Au₈⁺¹. Notwithstanding these differences, all metal clusters manifest signals at lower frequencies than Gly.

To observe the effect caused by the presence of metal clusters [Ag₈ and Au₈ (neutral, cationic, and anionic)] on the Raman spectra of Gly, the interaction was analyzed taking into account the entire range of neutral and anionic systems. This discussion poses an important question: whether threshold interaction energy is required for the SERS effect to occur. To correlate the binding energy with the Raman spectra, in Table 2 the binding energies for the reaction of metal clusters with Gly are presented. The corresponding chemical equation is also indicated.

Evidently, certain compounds manifest positive binding energy. This means that the products of the reaction are less stable than the dissociation limit, probably because there is a strong electrostatic repulsion. As compounds with positive binding energies are unlikely to be formed, thus the Raman spectra are not useful for these systems. For this reason, in the following, we report the Raman spectra for all those compounds manifesting negative binding energies, i.e. systems that are more stable than the dissociation limit.

Figures 3–5 present the optimized structures for all compounds with negative binding energies that were considered in this investigation, taking into account different pH values.

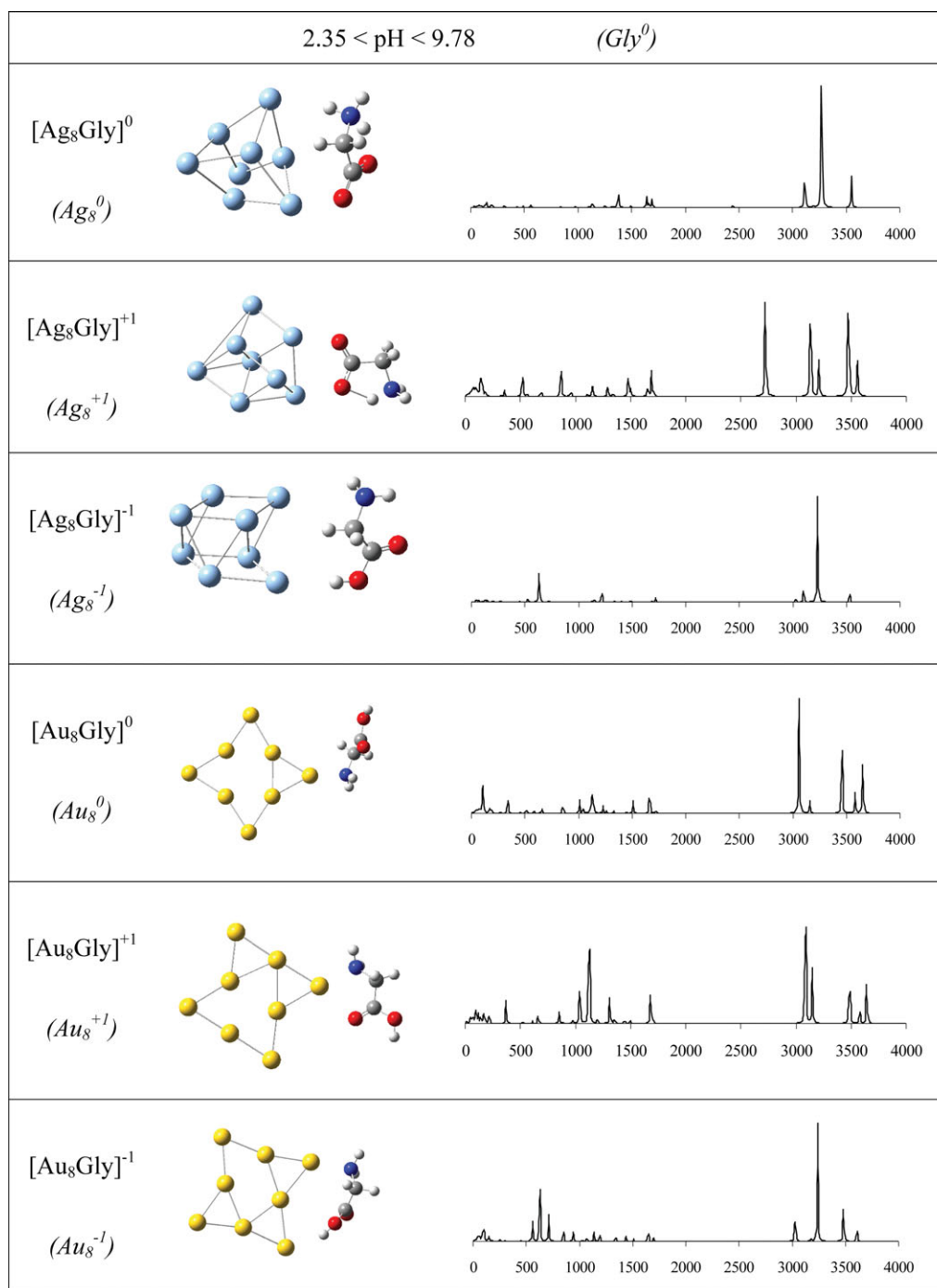


Figure 4. Optimized structures and simulated Raman spectra of Gly⁰ with Ag₈ and Au₈ (neutral, cationic, and anionic) Intensity of the Raman spectra in arbitrary units. [Color figure can be viewed in the online issue, which is available at wileyonlinelibrary.com.]

We include the molecular formula, the optimized structure, the metal cluster formula with the global charge, the Gly charge that was considered and the corresponding Raman spectra. The planarity of gold clusters disappears in two systems ([Au₈Gly]⁺¹ and [Au₈Gly]⁰), due to the interaction of Au₈⁰ and Au₈⁻¹ with Gly⁺¹. For the other systems containing gold, the planarity remains.

Figure 3 corresponds to Gly⁺¹, i.e., considering an acidic environment. Under these conditions (pH < 2.35), it is possible to see that the Raman spectra do depend on the charge of

the metal cluster. The spectra of neutral metal clusters are similar and correspondent mainly to the spectra of Gly⁺¹. The spectra of cationic clusters interacting with Gly⁺¹ are not included as these manifest positive binding energies. The Raman spectra of Gly⁺¹ interacting with silver and gold anionic clusters are different. The main bands of [Ag₈Gly]⁰ are located at 500–1500 cm⁻¹ whereas they are located at 1500, 3000 and 3600 cm⁻¹ for [Au₈Gly]⁰. These results concur with the idea that both the charge of the metal cluster at the surface, and the charge of the absorbed molecule are important.

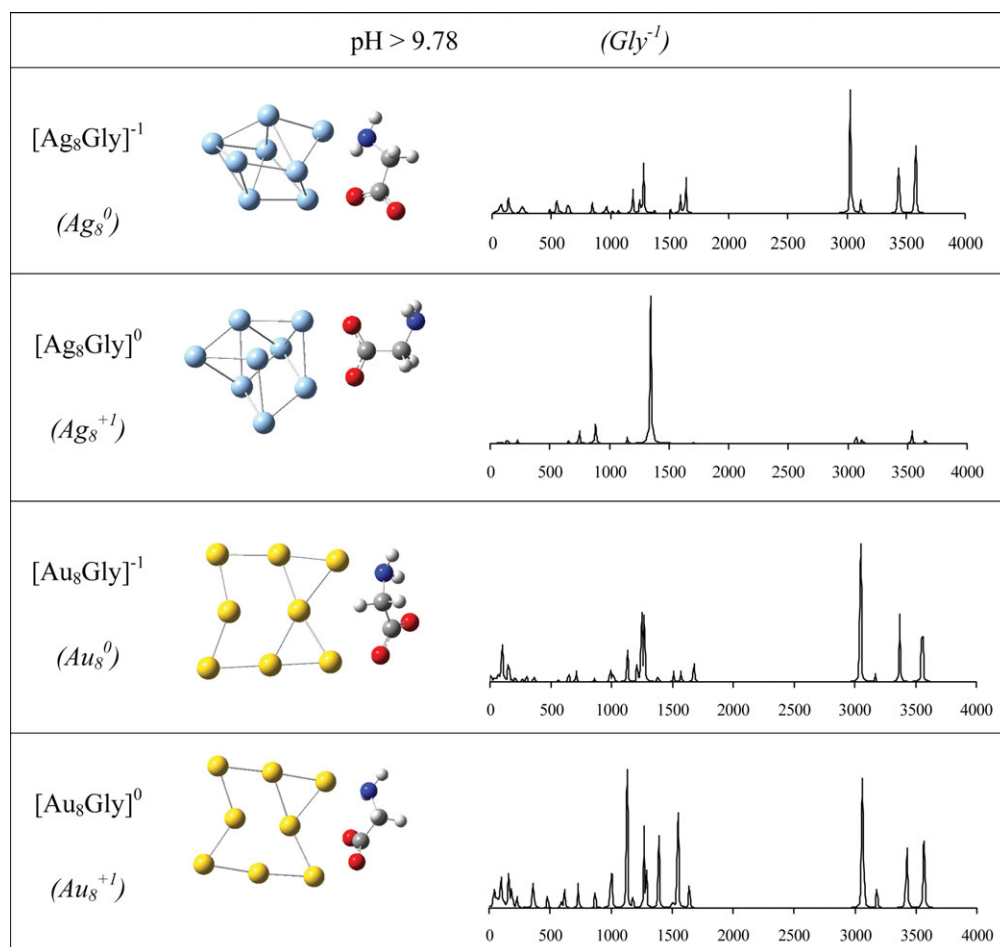


Figure 5. Optimized structures and simulated Raman spectra of Gly⁻¹ with Ag₈ and Au₈ (neutral, cationic, and anionic). Intensity of the Raman spectra in arbitrary units. [Color figure can be viewed in the online issue, which is available at wileyonlinelibrary.com.]

However, results are substantially different at neutral pH values (see Fig. 4) corresponding to Gly⁰. In Figure 4, all the spectra are quite similar. The main signals correspond to Gly⁰ and there are small bands for Au₈⁺¹ and Au₈⁻¹ at lower frequencies. In Figure 5, it is possible to see the results, assuming a basic setting (Gly is negatively charged). The Raman spectra also indicate the

dependence on the charge of the metal cluster. Neutral metal clusters mainly present the spectra of Gly⁻¹ with additional small bands at lower frequencies. Cationic metal clusters generate different results. The spectrum of [Ag₈Gly]⁰ presents an intense peak at 1400 cm⁻¹ and signals disappear at higher frequencies, whereas the spectrum of [Au₈Gly]⁰ presents several signals around 500–1500 cm⁻¹ and also shows several bands which may correspond to Gly⁻¹ at higher frequencies. The Raman spectra for anionic metal clusters are not presented, as the binding energy for these systems is positive.

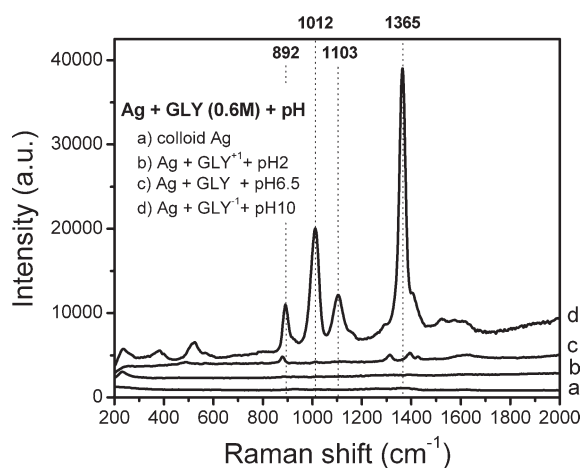


Figure 6. Experimental Raman spectra of Ag colloid and GLY at different pH values.

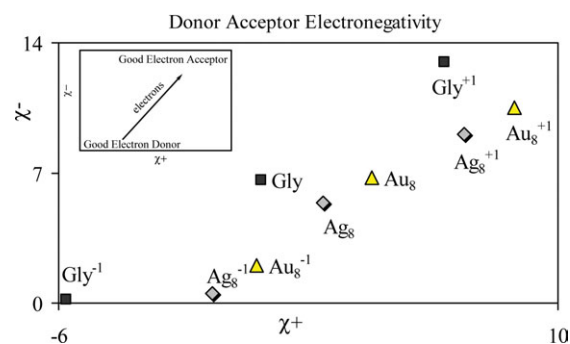


Figure 7. Results of χ^+ and χ^- . The small figure is the donor–acceptor electronegativity map. [Color figure can be viewed in the online issue, which is available at wileyonlinelibrary.com.]

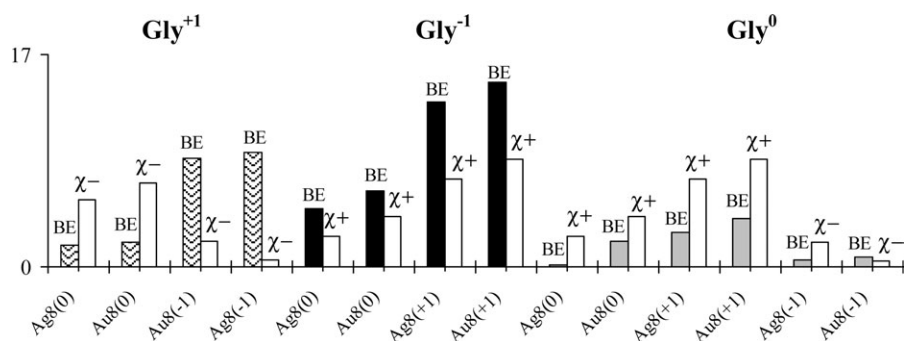


Figure 8. Binding energies (BE) of Table 2, χ^+ and χ^- of the metal clusters.

In summary, more intense bands of the Raman spectra appear at lower frequencies, when interactions occur between charge metal clusters and charge Gly molecule. The binding energy correlates well with the SERS effect, i.e., as the binding energy increases, the number and intensity of bands at lower frequencies in the Raman spectra also augment. It is important to note that in most cases, the interaction energy of the compounds presenting CE exceeds 30 kcal/mol. Apparently, for silver and gold clusters interacting with Gly, the threshold binding energy necessary for the appearance of the SERS effect is in the order of 30 kcal/mol.

To support these theoretical results, experimental Raman spectra of 0.6 M Gly in a silver colloid were recorded at different pH values. The results (Fig. 6) indicate that as the pH goes from acidic to basic an increase of the Gly Raman band intensities is observed. Under basic condition the spectrum presents intense bands around 800–1600 cm^{-1} , while either at acidic or neutral conditions the intensity of these bands becomes almost negligible. In other words, in the presence of colloidal Ag nanoparticles, the band intensities are strong for Gly⁻ (pH = 10) and very weak for Gly⁰ (pH = 6.5) and Gly⁺ (pH = 2).

Additionally, to complete the information about the experimental conditions, the Z potential of the colloidal silver was measured (Supporting Information Fig. 3S), which presents increasing negative values for pH going from acidic to basic conditions. At the present experimental conditions, this behavior indicates the affinity of the Ag nanoparticle surface for hydroxyl groups, which could be extrapolated to other anionic species such as Gly⁻. In terms of computational modeling, the anionic affinity of the Ag nanoparticle surface may be represented as a positive silver cluster such as Ag₈⁺. According to these results, a good agreement between theory and experiment is observed. In both cases the highest CE factor is obtained for anionic glycine (Gly⁻) interacting with positive charged Ag cluster (theory), or anionic glycine (Gly⁻) interacting with Ag nanoparticle surfaces presenting anionic affinity (experiment).

Other experimental results^[17] indicate that positive amino acids interact with the negatively charged gold surface yielding the SERS effect and this concurs with our results (see Fig. 3). Despite the differences between experiment and theory, as in the experiment there are silver or gold colloids or surfaces whereas in the calculations we considered metal clusters with only eight atoms, theory and experiment coincide in terms of the correlation between the global charge of the interacting systems and

the enhancement of the Raman spectra signals. All these results suggest that the electrostatic interaction between Gly and metal clusters represents an important factor for determining the intensity of the SERS signals.

Donor–acceptor electronegativity

To analyze the importance of the electrostatic interaction, the donor–acceptor electronegativity of the Gly molecule and the metal clusters (neu-

tral, anionic, and cationic) were obtained. These values are located on a “map” as indicated in the small box in Figure 7 to facilitate the analysis of results. A good electron donor is situated towards the bottom left, and a good electron acceptor is located towards the upper right of the figure. The electrons will go from the bottom left towards the upper right. Figure 7 also presents the donor–acceptor electronegativity for Gly and metal clusters.

The position on the map permits us to characterize the metal clusters and Gly as either electron donors or acceptors. It is clear that Gly⁻ is always an electron donor and a better electron donor (lower value of χ^-) than anionic metal clusters. Gly⁺ is a good electron acceptor but Ag₈⁺ and Au₈⁺ are better electron acceptors as their χ^+ is larger. Likewise, Gly⁺ is a very bad electron donor (the donor electronegativity χ^- is large) and Gly⁻ is a very poor electron acceptor (its acceptor electronegativity χ^+ is low). Neutral systems (Gly⁰, Ag₈⁰, and Au₈⁰) may act either as electron donors or electron acceptors, indicated by their location at the middle of the map. According to these results, the interaction between Gly⁻ and anionic metal clusters is not favorable, in accordance with the binding energies presented in Table 2. It is also evident, and to some extent logical, that the cationic metal clusters will not interact with Gly⁺. This is consistent with their position on the map as they are located very close to each other, whereas evidently the interaction will improve (more negative binding energies) where systems are further removed from each other on the map. For the neutral systems it is possible to see that Ag₈⁰ is closer to Gly⁰ than Au₈⁰, and that binding energy is less in silver than it is for gold. Anionic clusters are very close to Gly⁰ and both present diminished binding energies.

The binding energy is directly related to the charge transfer process. In terms of our indicators (χ^- and χ^+) this means that it must be directly connected with χ^+ and inversely correlated with χ^- . In Figure 8, we report the binding energies and the indicators (χ^- and χ^+). We used the indicator corresponding to the reaction which we intended to analyze. In Gly⁺, neutral and anionic metal clusters are electron donors, and a veritable inverse correlation between BE and χ^- of the metal clusters is evident. Gly⁻ acts as an electron donor, and therefore metal clusters (neutral and cation) must represent good electron acceptors. In this case, the BE in the reaction is directly related to the χ^+ of the metal clusters. Finally, Gly⁰ can either be an electron donor (when the interaction is with neutral and

cationic clusters), but likewise an electron acceptor (when the interaction is with anionic metal clusters). The indicators χ^+ and χ^- are directly and inversely correlated with the BE in each case.

In summary, χ^- and χ^+ are good parameters for the analysis of the charge transfer process. For the systems that we present here, CE is more intense for those systems with greater negative BE and the BE is more negative when there is a large charge transfer. Therefore, χ^- and χ^+ are good indicators of CE. The results reported here indicate that χ^- and χ^+ are good indicators, as metals can be either electron donors or acceptors as indicated previously in this paper as well as by other authors. For these two indicators, it is not necessary to obtain the energy gap and this is an advantage since electronic structure methods underestimate this value. Besides this, χ^- and χ^+ consider *I* and *A* together, which is important for these systems because a fractional charge transfer reaction takes place. The donor–acceptor electronegativity represents good parameters for providing useful information with which to design new molecules or new metal clusters which may display strong CE.

Conclusions

The electrostatic interaction between Gly and metal clusters represents an important factor for determining the intensity of the SERS signals. For the systems we present here, CE is more intense for those systems manifesting more negative BE, and the minimum interaction energy that is required for the SERS to take place is in the order of 30 kcal/mol.


The donor–acceptor electronegativity (χ^- and χ^+) are good indicators of CE, which may provide helpful information for the future design of novel molecules and metal clusters, possibly displaying strong CE.

Acknowledgments

This study was made possible due to the resources provided by the Instituto de Investigaciones en Materiales IIM. This work was carried out using a KanBalam supercomputer, provided by DGTIC, UNAM. The authors thank Caroline Karlake (Masters, Social Anthropology, Cambridge University, England) for reviewing the grammar and style of the text in English. They also acknowledge Oralia L. Jiménez, María Teresa Vázquez, Caín González Sánchez, and Joaquín Morales Rosales for their technical support.

Keywords: electrodonating · electroaccepting · charge transfer · density functional theory · metal clusters · Raman · SERS · chemical mechanism

How to cite this article: FJ. Tenorio, R. Sato-Berrú, JM. Saniger, A. Martínez, *Int. J. Quantum Chem.* **2012**, *112*, 3516–3524. DOI: 10.1002/qua.24153

 Additional Supporting Information may be found in the online version of this article.

- [1] (a) M. Fleischman, P. J. Hendra, A. McQuillan, *J. Chem. Phys.* **1974**, *26*, 163; (b) D. L. Jeanmaire, R. P. Van Duyne, *J. Electroanal. Chem.* **1977**, *84*, 1; (c) M. G. Albrecht, J. A. Crieghton, *J. Am. Chem. Soc.* **1977**, *99*, 5215.
- [2] S. Nie, S. R. Emory, *Science* **1997**, *275*, 1102.
- [3] K. Kneipp, H. Kneipp, G. Dinum, I. Itzkan, R. R. Dassari, M. S. Feld, *Appl. Spectrosc.* **1998**, *52*, 175.
- [4] M. Moskovits, J. S. Suh, *J. Phys. Chem.* **1984**, *88*, 5526.
- [5] J. S. Suh, M. Moskovits, *J. Am. Chem. Soc.* **1986**, *108*, 4711.
- [6] S. K. Kim, T. H. Joo, S. W. Suh, M. S. Kim, *J. Raman Spectrosc.* **1986**, *17*, 381.
- [7] F. Ni, R. Sheng, T. M. Cotton *Anal. Chem.* **1990**, *62*, 1958.
- [8] T. M. Herne, A. M. Ahern, R. L. Garrell, *J. Am. Chem. Soc.* **1991**, *113*, 846.
- [9] K. Sokolov, P. Hodorchenko, A. Petukhov, L. Nabiev, G. Chumanov, T. M. Cotton, *Appl. Spectrosc.* **1993**, *47*, 515.
- [10] K. Kneipp, R. R. Dasari, Y. Wang, *Appl. Spectrosc.* **1994**, *48*, 951.
- [11] T. Vo-Dinh, K. Houck, D. L. Stokes, *Anal. Chem.* **1994**, *66*, 3379.
- [12] N. R. Isola, D. L. Stokes, T. Vo-Dinh, *Anal. Chem.* **1998**, *70*, 1352.
- [13] X. Dou, T. Takama, Y. Yamaguchi, K. Hirai, H. Yamamoto, S. Doi, Y. Ozaki, *Anal. Chem.* **1997**, *69*, 1492.
- [14] X. Dou, T. Takama, Y. Yamaguchi, K. Hirai, H. Yamamoto, S. Doi, Y. Ozaki, *Appl. Opt.* **1998**, *37*, 759.
- [15] P. C. Lee, D. Meisel, *J. Phys. Chem.* **1982**, *86*, 3391.
- [16] S. Stewart, P. M. Fredericks, *Spectrochim. Acta Part A* **1999**, *55*, 1641.
- [17] H. Zhao, B. Yuan, X. Dou, *J. Opt. A: Pure Appl. Opt.* **2004**, *6*, 900.
- [18] X. Dou, Y. M. Jung, Z.-Q. Cao, Y. Ozaki, *Appl. Spectrosc.* **1999**, *53*, 1440.
- [19] K.-H. Chao, J. Choo, A.-W. Joo, *J. Mol. Struct.* **2005**, *738*, 9.
- [20] A. Kandakkathara, I. Utkin, R. Fedosejevs, *Phys. Status Solid C* **2009**, *6*, S27.
- [21] E. Podstawka-Proniewicz, M. Andrzejak, P. Kafarski, Y. Kim, L. M. Proniewicz, *J. Raman Spectrosc.* **2011**, *42*, 958.
- [22] G. Diaz-Fleming, F. Célis, C. Fredes, M. Campos-Vallette, A. E. Aliaga, R. Koch, *J. Raman Spectrosc.* **2010**, *41*, 160.
- [23] C. Garrido, A. E. Aliaga, J. S. Gomez-Jeria, R. E. Clavijo, M. M. Campos-Vallette, S. Sanchez-Cortes, *J. Raman Spectrosc.* **2010**, *41*, 1149.
- [24] N. Biswas, S. Thomas, A. Sarkar, T. Mukherjee, S. Kapoor, *J. Phys. Chem. C* **2009**, *113*, 7091.
- [25] I. B. Cozar, L. Szabó, D. Mare, N. Leopold, L. David, V. Chis, *J. Mol. Struct.* **2011**, *993*, 243.
- [26] (a) M. Moskovits, *Rev. Mod. Phys.* **1985**, *57*, 783; (b) M. Moskovits, *J. Raman Spectrosc.* **2005**, *36*, 485.
- [27] L. Jensen, C. M. Aikens, G. C. Schatz, *Chem. Soc. Rev.* **2008**, *37*, 1061.
- [28] (a) J. R. Lombardi, R. L. Birke, *J. Phys. Chem. C* **2008**, *112*, 5605; (b) J. R. Lombardi, R. L. Birke, *Acc. Chem. Res.* **2008**, *42*, 734.
- [29] M. Morton, L. Jensen, *J. Am. Chem. Soc.* **2009**, *131*, 4097.
- [30] (a) J. L. Gázquez, A. Cedillo, A. Vela, *J. Phys. Chem. A* **2007**, *111*, 1966; (b) J. L. Gázquez, *J. Mex. Chem. Soc.* **2008**, *52*, 3; (c) J. Z. Ramírez-Ramírez, R. Vargas, J. Garza, J. L. Gázquez, *J. Phys. Chem. A* **2010**, *114*, 7945.
- [31] W. Kohn, A. D. Becke, R. G. Parr, *J. Phys. Chem.* **1996**, *100*, 12974.
- [32] P. Hohenberg, W. Kohn, *Phys. Rev.* **1964**, *136*, B864.
- [33] W. Kohn, L. Sham, *J. Phys. Rev.* **1965**, *140*, A1133.
- [34] M. J. Frisch, G. W. Trucks, H. B. Schlegel, G. E. Scuseria, M. A. Robb, J. R. Cheeseman, G. Scalmani, V. Barone, B. Mennucci, G. A. Petersson, H. Nakatsuji, M. Caricato, X. Li, H. P. Hratchian, A. F. Izmaylov, J. Bloino, G. Zheng, J. L. Sonnenberg, M. Hada, M. Ehara, K. Toyota, R. Fukuda, J. Hasegawa, M. Ishida, T. Nakajima, Y. Honda, O. Kitao, H. Nakai, T. Vreven, J. A. Montgomery, Jr., J. E. Peralta, F. Ogliaro, M. Bearpark, J. J. Heyd, E. Brothers, K. N. Kudin, V. N. Staroverov, R. Kobayashi, J. Normand, K. Raghavachari, A. Rendell, J. C. Burant, S. S. Iyengar, J. Tomasi, M. Cossi, N. Rega, J. M. Millam, M. Klene, J. E. Knox, J. B. Cross, V. Bakken, C. Adamo, J. Jaramillo, R. Gomperts, R. E. Stratmann, O. Yazyev, A. J. Austin, R. Cammi, C. Pomelli, J. W. Ochterski, R. L. Martin, K. Morokuma, V. G. Zakrzewski, G. A. Voth, P. Salvador, J. J. Dannenberg, S. Dapprich, A. D. Daniels, O. Farkas, J. B. Foresman, J. V. Ortiz, J. Cioslowski, D. J. Fox, Gaussian 09, Revision A.02, Gaussian, Inc., Wallingford CT, **2009**.
- [35] A. D. Becke, *Phys. Rev. A* **1988**, *38*, 3098.
- [36] B. Mielich, A. Savin, H. Stoll, H. Peuss, *Chem. Phys. Lett.* **1989**, *157*, 200.
- [37] C. Lee, W. Yang, R. G. Parr, *Phys. Rev. B* **1988**, *37*, 785.
- [38] (a) P. J. Hay, W. R. Wadt, *J. Chem. Phys.* **1985**, *82*, 270; (b) P. J. Hay, W. R. Wadt, *J. Chem. Phys.* **1985**, *82*, 299.

- [39] W. R. Wadt, *J. Chem. Phys.* **1985**, *82*, 284.
- [40] T. H. Dunning, P. J. Hay, *Modern Theoretical Chemistry*; H. F. Schaefer, III, Ed.; Plenum: New York, **1976**; pp. 1–28.
- [41] O. V. Shishkin, L. Gorb, A. V. Luzanov, M. Elstner, S. Suhai, J. Leszczynski, *J. Mol. Struct. (Theochem)* **2003**, *625*, 295.
- [42] C. Møller, M. S. Plesset, *Phys. Rev.* **1934**, *46*, 1618.
- [43] S. Saebo, J. Almlof, *Chem. Phys. Lett.* **1989**, *154*, 83.
- [44] S. Bulusu, X. Li, L.-S. Wang, X. C. Zeng, *Proc. Natl. Acad. Sci. USA* **2006**, *103*, 8326.
- [45] (a) A. Martínez, *J. Phys. Chem. A.* **2009**, *113*, 1134; (b) J. Valdespino-Saenz, A. Martínez, *J. Mol. Struct. (Theochem)* **2010**, *393*, 34.
- [46] A. Martínez, *J. Phys. Chem. C* **2010**, *114*, 21240.

Received: 27 February 2012
Revised: 9 April 2012
Accepted: 10 April 2012
Published online on 11 May 2012
